Electronic Supplementary Information

for

Cytotoxic tantalum(V) half-sandwich complex: a new challenge for metal-based anticancer agents

Pavel Štarha, Zdeněk Trávníček* and Zdeněk Dvořák

Division of Biologically Active Complexes and Molecular Magnets, Regional Centre of Advanced Technologies and Materials, Faculty of Science, Palacký University in Olomouc, Šlechtitelů 27, 783 71 Olomouc, Czech Republic

Corresponding Author (Z.T.):

* E-mail: zdenek.travnicek@upol.cz.

Table of contents

Experimental section 2
Results and discussion 10
Figure S1–S10 11
Table S1–S12 21
References 34

Experimental Section

Materials

The chemicals [Ta(η^5-Cp*)Cl_4] (Cp* = pentamethylcyclopentadienyl), 2-hydroxybenzaldehyde (salicylaldehyde), 2-aminophenol, silver(I) nitrate, (*SP*-4-2)-diammine-dichloridoplatinum(II) (*cisplatin*), *staurosporine*, reduced glutathione (GSH), guanosine 5′-monophosphate disodium salt hydrate (GMP), L-cysteine (CSH), L-tryptophan (Try), ammonium formate (for HPLC), solvents propan-2-ol, diethyl ether, dichloromethane, *n*-hexan, dimethyl sulfoxide (DMSO), *N*,*N*-dimethylformamide (DMF), methanol (MeOH), acetonitrile (ACN), deuterated solvents (DMSO-d_6, DMF-d_7, $DClO_4$ and KOD) and HPLC grade solvents (acetonitrile, water) were supplied by VWR International (Stříbrná Skalice, Czech Republic), Sigma-Aldrich (Prague, Czech Republic), Fisher Scientific (Pardubice, Czech Republic) and Litolab (Chudobín, Czech Republic). All the chemicals and solvents were used without further purification. Roswell Park Memorial Institute (RPMI-1640) medium, trypsin, Dulbecco's Modified Eagle's Medium (DMEM), tris(hydroxymethyl)aminomethane hydrochloride (Tris-HCl) and phosphate-buffered saline (PBS) were purchased from Sigma-Aldrich and Fisher Scientific.

Syntheses

2-{(*E*)-[(2-hydroxyphenyl)imino]methyl}phenol (H_2salaph). The Schiff base H_2salaph was prepared in the microwave reactor (1 min, 100 °C, propan-2-ol) using the modification of the reported procedure.[1] *Anal.* Calcd. for $C_{13}H_{11}NO_2$: C, 73.2; H, 5.2; N, 6.6; found: 72.7; H, 5.6; N, 6.2 %. ^{1}H NMR (DMSO-d_6, 300 K, ppm): δ 13.80 (s, 1H, O1–H), 9.74 (s, 1H, O9–H), 8.96 (s, 1H, C7–H), 7.61 (d, *J* = 8.2 Hz, 1H, C3–H), 7.37 (m, 2H, C5–H, C13–H), 7.13 (t, *J* = 7.8 Hz, 1H, C11–H), 6.95 (m, 3H, C4–H, C6–H, C10–H), 6.88 (t, *J* = 7.8 Hz, 1H, C12–H). ^{13}C NMR (DMSO-d_6, 300 K, ppm): δ 161.7 (C7–H), 160.7 (C1), 151.1 (C9), 135.0 (C8), 132.9 (C5–H), 132.3 (C3–H), 128.1 (C11–H), 119.6–119.5 (C2, C12–H, C13–H), 118.8 (C10–H), 116.7–116.5 (C4–H, C6–H).

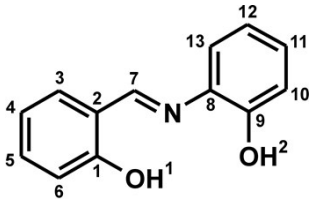

Complex [Ta(η^5-Cp*)Cl_2(salaph)] (1). The starting Ta(V) complex [Ta(η^5-Cp*)Cl_4] (0.1 mmol) and the Schiff base H_2salaph (0.1 mmol) were suspended in 5 mL of dichloromethane and the mixture was stirred for 1 min at 100 °C and 6 bar using the microwave reactor. The obtained dark red solution was cooled to ambient temperature

and the solvent volume was reduced to *ca.* 1 mL. The precipitation of the dark red product was induced by the addition of an excess of *n*-hexane. The obtained solid was removed by filtration, washed by diethyl ether (3 × 0.5 mL) and dried for 30 min in desiccator under vacuum. A yield was 60%. *Anal*. Calcd. for $C_{23}H_{24}NCl_2O_2Ta$: C, 46.2; H, 4.0; N, 2.3; found: C, 46.3; H, 4.0; N, 2.0 %. ^{1}H NMR (DMSO-d_6, 300 K, ppm): δ 8.85 (s, 1H, C7–H), 7.64 (d, *J* = 8.3 Hz, 1H, C13–H), 7.53 (d, *J* = 6.4 Hz, 1H, C3–H), 7.46 (t, *J* = 7.8 Hz, 1H, C5–H), 7.12 (t, *J* = 7.8 Hz, 1H, C11–H), 6.93 (t, *J* = 7.4 Hz, 1H, C4–H), 6.82 (t, *J* = 7.8 Hz, 1H, C12–H), 6.57 (d, *J* = 8.3 Hz, 1H, C6–H), 6.47 (d, *J* = 8.3 Hz, 1H, C10–H), 2.28 (s, 15H, C20–24–H). ^{13}C NMR (DMSO-d_6, 300 K, ppm): δ 158.6 (C9), 157.9 (C1), 154.8 (C7–H), 138.0 (C8), 137.0 (C5–H), 135.2 (C3–H), 130.4 (C11–H), 126.8 (C15–C19), 122.8 (C2), 122.1 (C4–H), 121.8 (C12–H), 120.2 (C6–H), 117.9 (C10–H), 116.9 (C13–H), 11.8 (C20–C24–H). ESI+ MS (ACN): 562.2 (calc. 562.1; 100%; $[Ta(Cp^*)(salaph)Cl]^+$). IR (ν_{ATR}/cm^{-1}): 3075w, 2985w, 2917m, 1616s, 1589ms, 1556m, 1476s, 1447ms, 1385ms, 1325w, 1298s, 1254s, 1178w, 1152m, 1122m, 1073w, 1030m, 963w, 942w, 926m, 858ms, 797m, 768ms, 737ms, 642m, 625m, 550m, 532m, 492w, 467w.

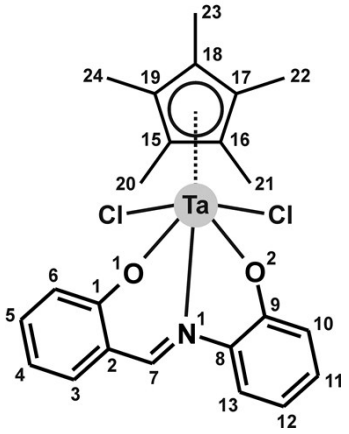

Complex $[Ta(\eta^5\text{-}Cp^*)(salaph)(OH_2)]^{2+}$ (1-OH_2). For the HPLC experiments, the stoichiometric amount of $AgNO_3$ (dissolved in H_2O) was added to the ACN solution of complex **1** (1 mM final concentration) and the mixture was stirred for 1 h under the aluminium foil at ambient temperature. Thereafter, the formed AgCl was centrifuged and the solution the **1-OH_2** species in ACN/H_2O (1:1, *v/v*) was analysed as described elsewhere. Analogically, the **1-OD_2** species for NMR experiments (described elsewhere) was prepared in the mixture of DMF-d_7/D_2O (1:1, *v/v*).

Methods

The syntheses (see above) were performed in a Monowave 300 microwave reactor (Anton Paar), using the 30 mL vials for microwave synthesis equipped with magnetic stirring bar.

Elemental analyses (C, H, N) were carried out by a Flash 2000 CHNS Elemental Analyser (Thermo Scientific). ^{1}H, ^{13}C, ^{1}H–^{1}H gs-COSY, ^{1}H–^{13}C gs-HMQC and ^{1}H–^{13}C gs-HMBC spectra were recorded on the DMSO-d_6 solutions using a JEOL JNM-ECA 600II

spectrometer at 600.00 MHz (for ^{1}H) and 150.86 MHz (for ^{13}C). The obtained ^{1}H and ^{13}C NMR spectra were calibrated against the residual signals (2.50 ppm for ^{1}H NMR, 39.5 ppm for ^{13}C NMR) of the used solvent.[2] The splitting of the ^{1}H NMR signals is defined as s = singlet, d = doublet, t = triplet and m = multiplet. Mass spectrometry was performed on the ACN solution using a LCQ Fleet Ion Trap spectrometer (Thermo Scientific; Qual Browser software, version 2.0.7) in the positive electrospray ionization mode (ESI+). FTIR spectra were recorded by a Nexus 670 FT-IR spectrometer (Thermo Nicolet) using an ATR technique (the 400–4000 cm^{-1} region).

X-ray data collection of complex **1** was performed on a D8 QUEST diffractometer (Bruker) using a PHOTON 100 CMOS detector and Mo–Kα radiation (λ = 0.71073 Å). The data collection and reduction were performed using the APEX3 software package[3] and the structure was solved by a direct method (SHELXS) and refined with the Bruker SHELXTL Software Package.[4] The structural data was deposited in the Cambridge Crystallographic Data Centre under the accession number CCDC 1851694. The graphics were drawn and additional structural calculations were performed by DIAMOND[5] and Mercury[6] software. The crystal data and structure refinement can be found in Table S1.

A solubility of complex **1** was quantified by the addition of 0.5 mL of DMSO, ACN or MeOH, or 1 mL of PBS (pH 7.4), Tris-HCl (pH 7.4), DMEM or RPMI-1640 to *ca.* 3 mg of complex **1**, followed by 2 h of shaking at 20 °C. After that, all samples were centrifuged (10 min, 11,000 rpm) and supernatants were collected. Supernatants were 1000× diluted by 5% HNO_3 and the Ta content was assessed by ICP-MS (ICP-MS spectrometer 7700x, Agilent) by external calibration using the Tantalum Standard for ICP (TraceCERT®, 1000 mg/L Ta in HNO_3 and HF; Sigma-Aldrich). The obtained values were corrected for adsorption effects.

^{1}H NMR studies of hydrolysis

The appropriate amount (for 600 μL of 1 mM solutions in DMF-d_7/D_2O (1:1, *v/v*) of complex **1** was dissolved in DMF-d_7 (300 μL) and D_2O (300 μL) was added; *note:* DMF-d_7 was added due to low solubility of complex **1** in water and the amount of DMF-d_7 was optimized to keep the required concentration of complex **1** in solution. ^{1}H NMR spectra were recorded on the fresh solutions (t = 0 h), and after 0.5, 1, 2, 3, 4, 6, 24, 48 and 72 h of standing at ambient temperature or 37 °C. The obtained ^{1}H NMR spectra were

calibrated against the residual signal of DMF-d_7.[2] Analogical experiments were performed in the DMF-d_7/D_2O (7:3, *v/v*) and DMF-d_7/D_2O (9:1, *v/v*) mixtures at 37 °C.

For comparative purposes, the ^{1}H NMR spectra were also recorded for **1-OD$_2$** (at pH 7 and 4 (set by the addition of diluted $DClO_4$ in D_2O)), [Ta(η^5-Cp*)Cl_4], free H_2salaph as well as for salicylaldehyde and 2-aminophenol in the DMF-d_7/D_2O (1:1, *v/v*) mixture of solvents. *Note:* due to low water solubility, no attempts to evaluate the pK_a value of complex **1** were performed.

^{1}H NMR studies of interactions with biomolecules

The appropriate amounts (for 2 × 600 μL of 1 mM solutions) of complex **1** were dissolved in DMF-d_7 (300 μL) and the solutions of CSH, Try, GSH or GMP (5 mol equiv.) in D_2O (300 μL) were added. ^{1}H NMR spectra were recorded on the fresh solutions (t = 0 h), and after 0.5, 1, 2, 3, 4, 6, 24, 48 and 72 h of standing at 37 °C. The spectra were referenced against the residual signal of DMF-d_7.[2] For comparative purposes, the ^{1}H NMR spectrum was recorded also for free CSH, Try, GSH and GMP in the used medium.

HPLC studies

Reversed-phase high-performance liquid chromatography coupled to the positive electrospray ionization mode mass spectrometry (RP-HPLC/ESI+ MS) was carried out using UHPLC-MS (Dionex/Thermo Fisher Scientific) equipped with an ReproSil-Pur Basic C18 (5 μm pore size, 200 × 4.6 mm). The detection wavelength was 254 nm.

For determination of complex **1** purity (ACN solution, 1 mM concentration), pure ACN (HPLC grade) was used as the mobile phase.

For the hydrolysis studies, complex **1** (1 mM concentration) was dissolved in the mixture of 50% ACN/50% H_2O (*v/v*; HPLC grade) and the mixture of 0.1% ammonium formate in H_2O (A) and ACN (B) was used as the mobile phase at gradients of 10 % B (t = 0 min), 80 % B (t = 30 min), 80 % B (t = 40 min), 10 % B (t = 41 min) and 10 % B (t = 55 min) over a 55 min period (1 mL min^{-1} flow rate). For comparative purposes, the same experiment was performed also for **1-OH$_2$** in the same medium.

Stock solutions for the cell-based studies

The 100 mM stock solutions of complex **1** and the platinum reference drugs *cisplatin* and *oxaliplatin* (involved in the testing for comparative purposes) were prepared by dissolving of appropriate amounts of these agents in 500 μL of DMF.

Cell cultures

The A2780 human ovarian carcinoma cell line, A2780R *cisplatin*-resistant human ovarian carcinoma cell line, HOS human osteosarcoma cell line and MRC-5 human normal lung fibroblast cell line were supplied by the European Collection of Cell Cultures (ECACC), while the 96-well culture plate with the primary culture of human hepatocytes (Hep) was purchased from Biopredic Intl. The cells were cultured according to the suppliers´ instructions, using RPMI-1640 medium supplemented with 10% of fetal calf serum, 1% of 2 mM glutamine and 1% penicillin/streptomycin (for the A2780, A2780R, HOS and MRC-5 cells) and chemically defined medium consisting of a mixture of William´s E and Ham´s F-12 (1:1, *v/v*) (for the Hep cells), respectively. All cell lines were grown as adherent monolayers at 37 °C and 5% CO_2 in a humidified atmosphere.

In vitro cytotoxicity studies

Following the seeding at the 96-well culture plates, the A2780, A2780R, HOS and MRC-5 cells were allowed to stabilize for 24 h. Then, the cells were incubated for 24 h (A2780, A2780R, HOS) or 72 h (MRC-5) exposure time with complex **1** (0.1–50.0 μM concentrations for A2780, A2780R, HOS and MRC-5 cells and 0.1–100.0 μM concentration for Hep cells) as well as with 0.1% DMF (*v/v*; negative control), 1% Triton X-100 (*v/v*; positive control), and *cisplatin* (0.1–50.0 μM concentrations for A2780, A2780R, HOS and MRC-5 cells and 0.1–80.0 μM concentration for Hep cells) and *oxaliplatin* (0.01–25.0 μM concentrations) used as the reference drugs. After that, the solutions were removed, the cells were washed by the drug-free medium and the cell viability was assessed (see below).

In the case of the studies at the A2780 cells, the time-dependent experiments were performed for complex **1** and *cisplatin*, both applied also with the 48 h and 72 h exposure times.

Regarding the Hep cells, these were pre-incubated in drug-free medium at 37 °C for 24 h and then treated for the next 24 h at 37 °C with different concentrations of complex **1** and *cisplatin* prepared from their stock solutions by dilution with appropriate

medium. After 24 h drug exposure, the supernatants were removed and the cells were washed with drug-free PBS.

The cell viability was in all the above-described cases assessed by an MTT assay and evaluated spectrophotometrically at 540 nm using an Infinite 200 PRO microplate reader (Tecan Group Ltd., Männedorf, Switzerland). The data were expressed as the percentage of viability, where 100% and 0% represents the treatments with negative and positive controls, respectively. The data from the A2780, A2780R, HOS and MRC-5 cells were acquired from three independent experiments (conducted in triplicate) using cells from different passages, and the resulting IC_{50} values (μM) were calculated from the viability curves and the results are presented as arithmetic mean ± standard deviation (SD). The data from the Hep cells were acquired in triplicate.

Cellular accumulation

The A2780 cells were seeded in 6-well culture plates at a density of 1×10^6 cells per well and incubated overnight (37 °C and 5% CO_2 in a humidified incubator). Then, the cells were treated for 24 h by the IC_{50} concentration of complex **1** (and *cisplatin* for comparative purposes). Then the A2780 cells were washed with PBS (2 × 2 mL), harvested by the trypsinization, and centrifuged. The supernatants were discarded and the pellets were immediately digested in 500 μL of nitric acid (6 h, 70 °C), to give the fully homogenized solutions. The solutions were diluted with 4.5 mL of water and the Ta content was determined by ICP-MS (ICP-MS spectrometer 7700x, Agilent) by external calibration using the Tantalum Standard for ICP (TraceCERT®, 1000 mg/L Ta in HNO_3 and HF) and Transition metal mix 3 for ICP (TraceCERT®, 100 mg/L); Sigma-Aldrich. The obtained values were corrected for adsorption effects. The experiments were performed in triplicate and the results are presented as arithmetic mean ± SD.

Flow cytometry studies

The A2780 cells were seeded in 6-well culture plates at a density of 1×10^6 cells per well and incubated overnight (37 °C and 5% CO_2 in a humidified incubator). The cultured cells were harvested by trypsinization, washed with PBS, centrifuged, re-suspended in PBS, divided (individual samples count *ca.* 3×10^5 cells) and stained, as specified below. In all cases, complex **1** was applied at the IC_{50} concentration. The cells were analysed by a CytoFlex flow cytometer (Beckman Coulter) and the obtained data

were analysed using CytExpert™ software (Beckman Coulter). In all cases, the untreated stained A2780 cells were used as a negative control. All experiments were carried out in triplicate (*ca.* 3×10^5 cells per sample).

Cell cycle studies. The A2780 cells (treated for 24 h) were stained for 30 min at 25 °C by a propidium iodide (PI) supplemented with RNase A and 0.1% (*v/v*) Triton X-100. After that, the DNA content was assessed using flow cytometry detecting emission at 617 nm after excitation at 535 nm. The A2780 cells treated by *cisplatin* (IC_{50} concentration) were involved for comparative purposes.

Induction of apoptosis. After the 24 h long treatment, the A2780 cells were processed following the instructions supplied in Annexin V-FITC Apoptosis Detection Kit (Enzo Life Sciences). The cells treated by the apoptosis-inductor *staurosporine* (1 μg/mL) were involved in the study as the positive control. Flow cytometry was performed using a blue laser (488 nm) and 525/40 BP and 610/20 BP filters. *Cisplatin* was involved for comparative purposes.

ROS/Superoxide assay. The A2780 cells (24 h exposure) were stained according the manufacturer´s instruction using the orange/green fluorescent reagents supplied at the Total ROS/Superoxide detection kit (Enzo Life Sciences). The cells treated with *pyocyanin* were used as the positive control. Cells were analysed by flow cytometry detecting emissions at 525 nm (total oxidative stress) and 620 nm (superoxide).

Mitochondrial membrane potential assay. The A2780 cells were treated for 24 h and then processed according the MITO-ID® Membrane potential detection kit (emission maxima at 590 and 525 nm for the orange and green dyes, respectively; Enzo Life Sciences). The stained cells treated with carbonyl cyanide 3-chlorophenylhydrazone (CCCP; 2 μM final concentration) were used as the positive control. The A2780 cells treated by *staurosporine* (1 μg/mL concentration) and *cisplatin* (IC_{50} concentration) were involved in this experiment for comparative purposes.

Cytochrome *c* release. The cell staining procedure was performed according the instructions supplied in the FlowCellect™ Cytochrome *c* Kit (Millipore, Catalog No. FCCH100110) containing the Anti-IgG1-FITC Isotype Control (positive control) and Anti-Cytochrome c-FITC Antibody dye. For this experiment, the apoptosis inducer *staurosporine* (1 μg/mL concentration) and *cisplatin* (IC_{50} concentration) were involved for comparative purposes as well.

Statistical analysis

An ANOVA test was used for statistical analysis with the values of $p < 0.05$ (*), 0.01 (**) and 0.005 (***) considered to be statistically significant. QC Expert 3.2 Statistical software (TriloByte Ltd.) was used to perform the analysis.

Results and discussion

Proposed mechanism of action

Complex **1** induced apoptosis and depletion of mitochondrial membrane potential connected with a release of pro-apoptotic protein cytochrome c into the cytosol of the treated A2780 ovarian carcinoma cells (Table S8–S11). Although apoptosis is usually connected with an increase of sub-G_1 cell cycle phase population as a consequence of DNA fragmentation,[7] as it is known for *cisplatin*,[8] it was not observed for Ta(V) complex **1**. Specifically, A2780 cells treated by complex **1** showed similar sub-G_1 cell population as the negative control, but markedly lower as compared with *cisplatin* (Table S8). This observation implies that mechanism of action of complex **1** is most likely different from *cisplatin*.

An induction of apoptosis that is not connected with a relevant sub-G_1 population of the treated cancer cells has been reported for various cytotoxic agents, such as known apoptosis-inducer *staurosporine*[9] or half-sandwich Os(II) complex [Os(η^6-*p*cym)(L)I]PF_6, where *p*cym = *p*-cymene and L = 4-(2-pyridylazo)-*N*,*N*-dimethylaniline.[10] Thus, the preliminary mechanistic results reported in this work for complex **1** indicated that the mechanism of action is likely to be more similar to that of complex [Os(η^6-*p*cym)(L)I]PF_6 than to that of conventional *cisplatin*. This hypothesis is supported by other results obtained for complex **1** that resembles complex [Os(η^6-*p*cym)(L)I]PF_6, in particular a considerable intracellular induction of reactive oxygen species (ROS). On the other hand, the results of the interaction studies with GMP (*i.e.*, no interaction of complex **1** with GMP) indicated that DNA is probably not an intracellular target for the discussed Ta(V) complex **1**, which again pointed out mechanistic difference against *cisplatin*, whose mechanism of action is based on covalent interaction with guanines of nuclear DNA molecule.[11] Thus, it seems that complex **1** aims different intracellular targets than *cisplatin*, as it was described for another half-sandwich Ru(II) complex containing various pyridinecarbothioamides.[12] In particular, these complexes showed high *in vitro* cytotoxicity connected with selective targeting of plectin, a key protein for cytoskeleton, whose dysfunction results in serve abnormalities of various cells (*e.g.*, skin) including cancer ones.[13] Thus a specific protein targeting has to be taken into account as possibly involved in mechanism of action of complex **1**.

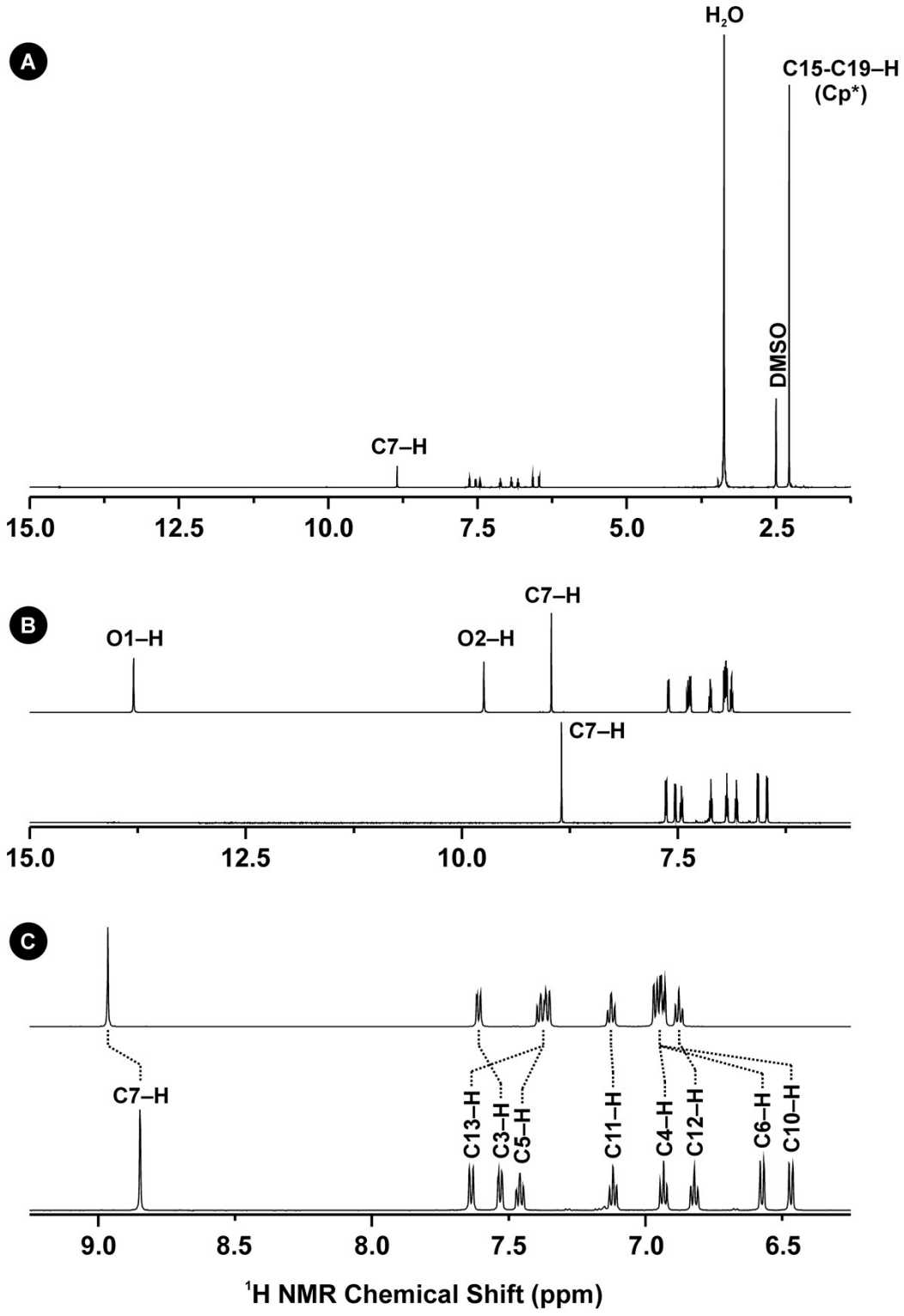

Figure S1. ^{1}H NMR spectra (depicted at three different ranges) of complex **1** (A, B bottom, C bottom) and free H_2salaph (B top and C top), both dissolved in DMSO-d_6.

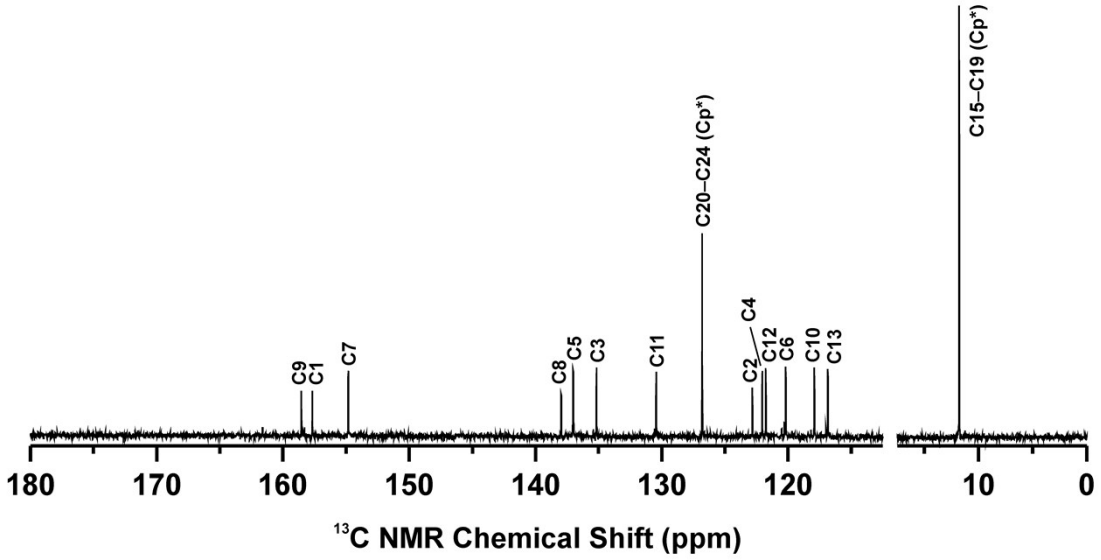

Figure S2. ^{13}C NMR spectrum of complex **1** dissolved in DMSO-d_6.

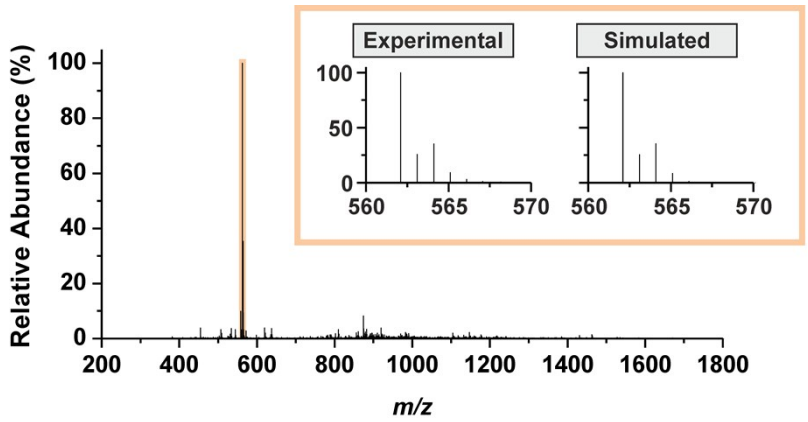

Figure S3. ESI+ mass spectrum of complex [Ta(η^5-Cp*)(salaph)Cl$_2$] (**1**) dissolved in acetonitrile (recorded in the 150–1800 *m/z* range) given with the comparison of the experimental and simulated isotopic distribution of the [Ta(η^5-Cp*)(salaph)Cl]$^+$ species.

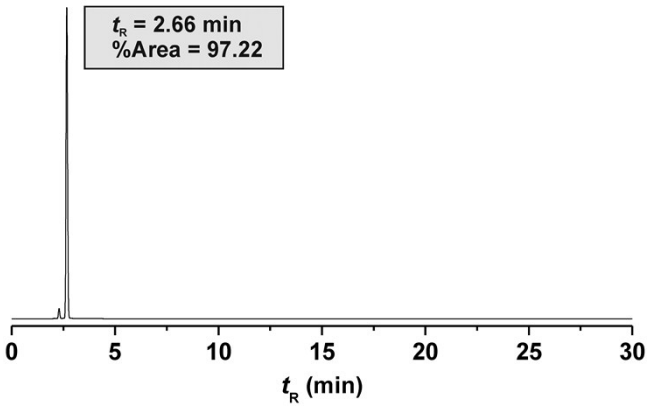

Figure S4. The results of RP-HPLC coupled with ESI+ mass spectrometry of complex **1** dissolved in ACN and using ACN as a mobile phase, showing the dominant RP-HPLC peak at t_R = 2.66 min with 97.22 %Area. The coupled ESI+ mass spectrum of this peak showed the peak of the $[Ta(\eta^5\text{-}Cp^*)(salaph)Cl]^+$ species (562.1 *m/z*).

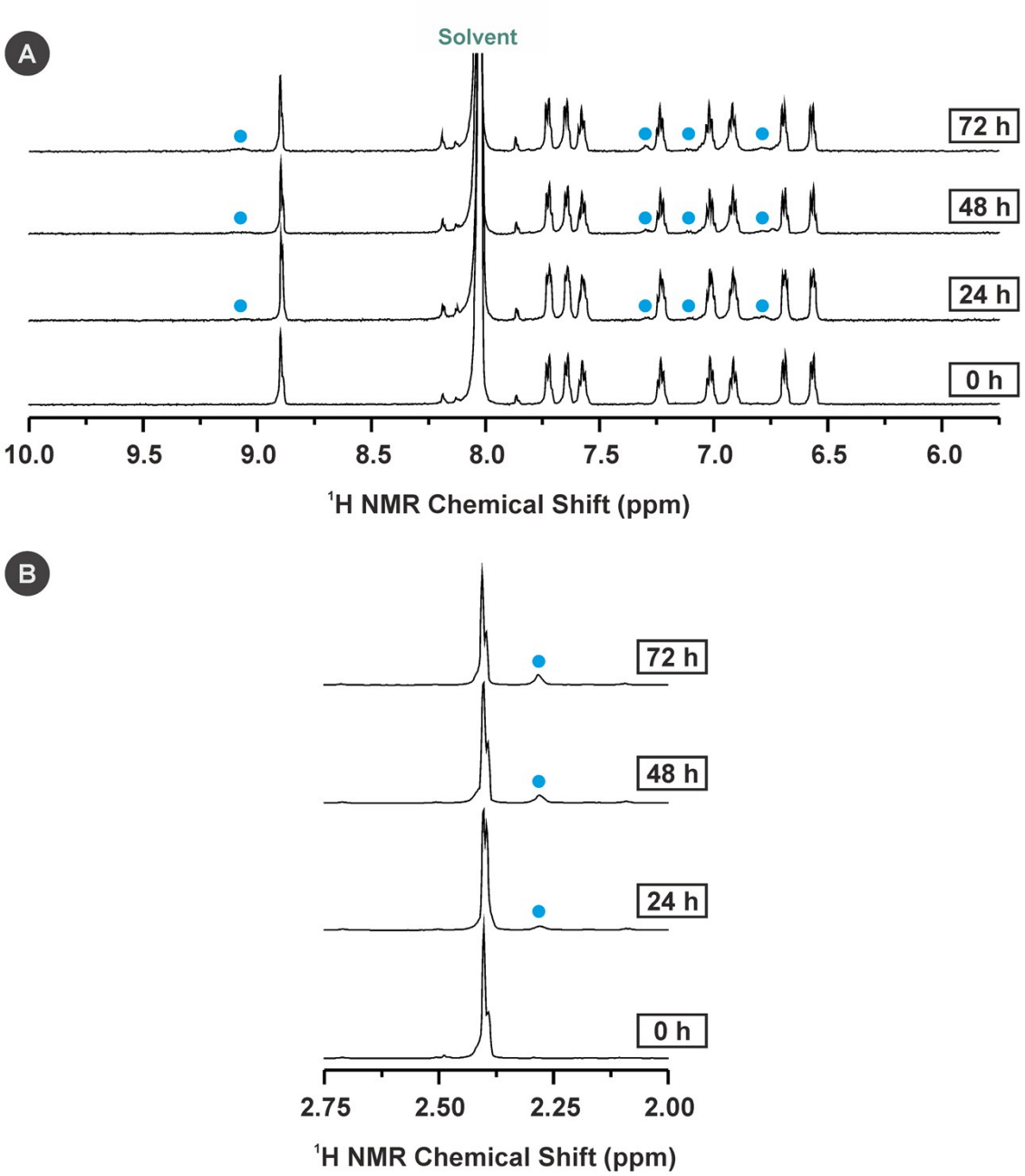

Figure S5. A comparison of the ^{1}H NMR spectra (5.75–10.00 ppm (A) and 2.00–2.75 ppm (B) regions) of complex **1** dissolved in the mixture of 50% DMF-d_7/50% D_2O, as observed at different time points up to 72 h of standing at ambient temperature. The signals labelled with blue spheres belong to hydrolysate.

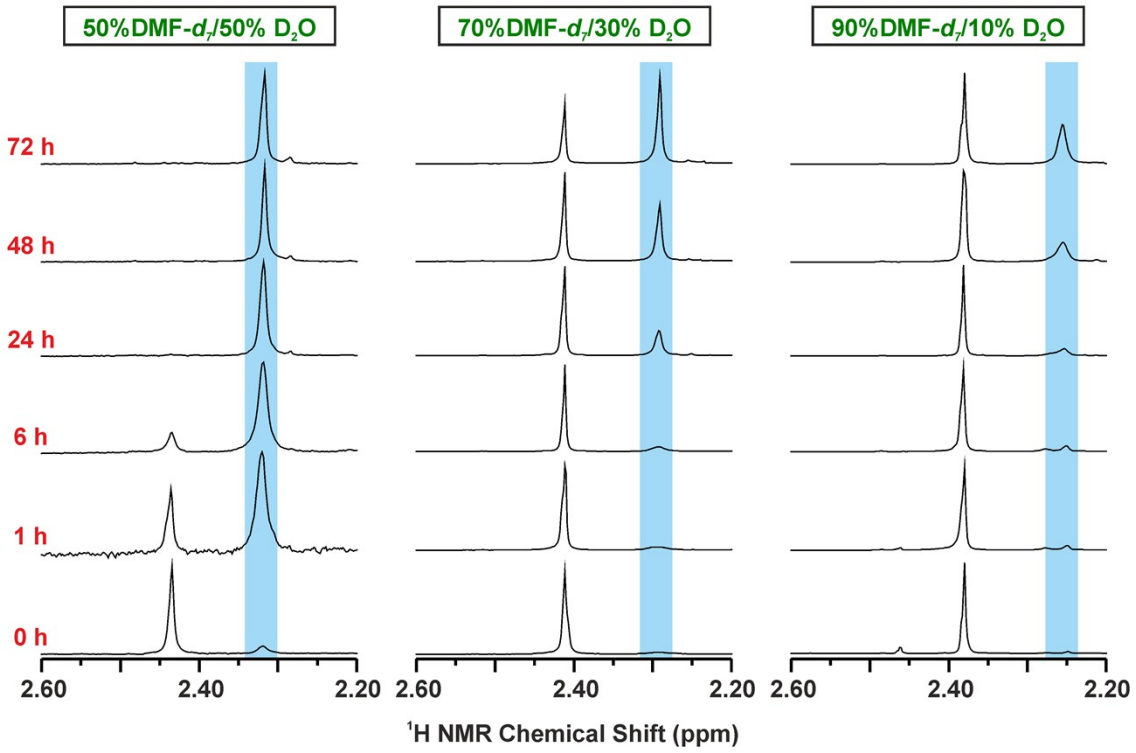

Figure S6. The representative parts (a Cp* ligand singlet) of the ^{1}H NMR spectra of complex **1** in 50% DMF-d_7/50% D_2O (*left*), 70% DMF-d_7/30% D_2O (*middle*) and 90% DMF-d_7/10% D_2O (*right*) at various time points. The spectra were recorded at 37 °C.

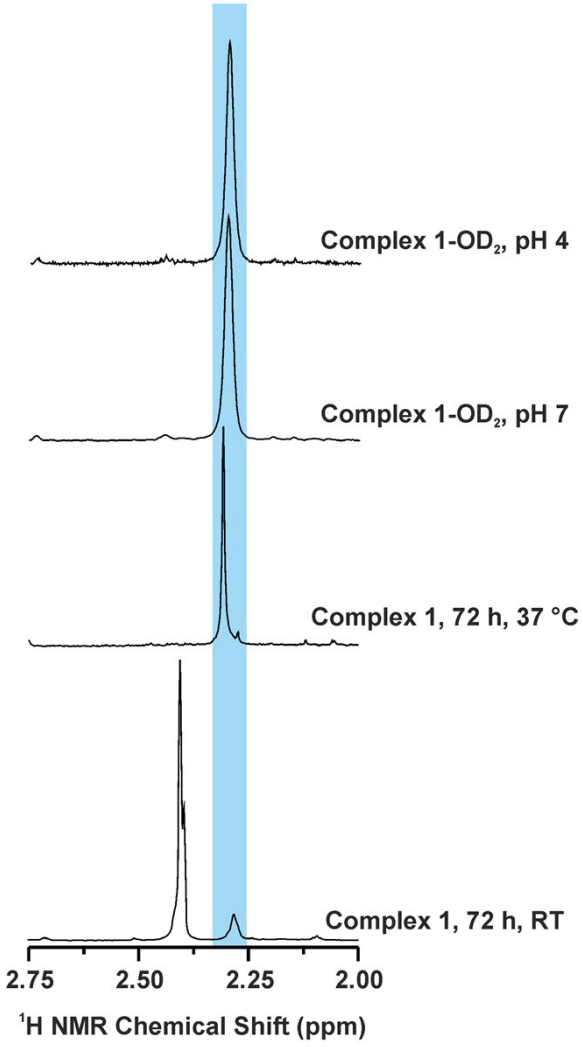

Figure S7. The representative parts of the ^{1}H NMR spectra (50% DMF-d_7/50% D_2O) showing the ^{1}H NMR signals of the methyl groups of the Cp* ligand of complex **1** (after 72 h of standing at ambient temperature (RT) or 37 °C) and the **1-OD$_2$** species as observed at pH of *ca.* 7 and 4.

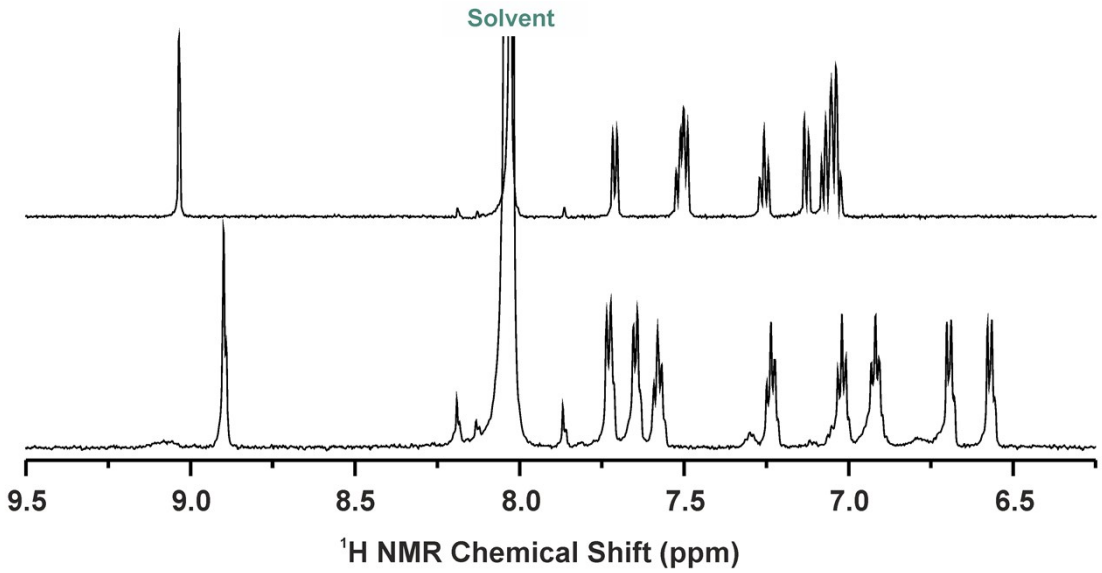

Figure S8. A comparison of the ^{1}H NMR spectra (6.25–9.50 ppm region) of complex **1** dissolved in the mixture of 50% DMF-d_7/50% D_2O for 72 h at 37 °C (*bottom*) and free H_2salaph dissolved in the same medium (*top*).

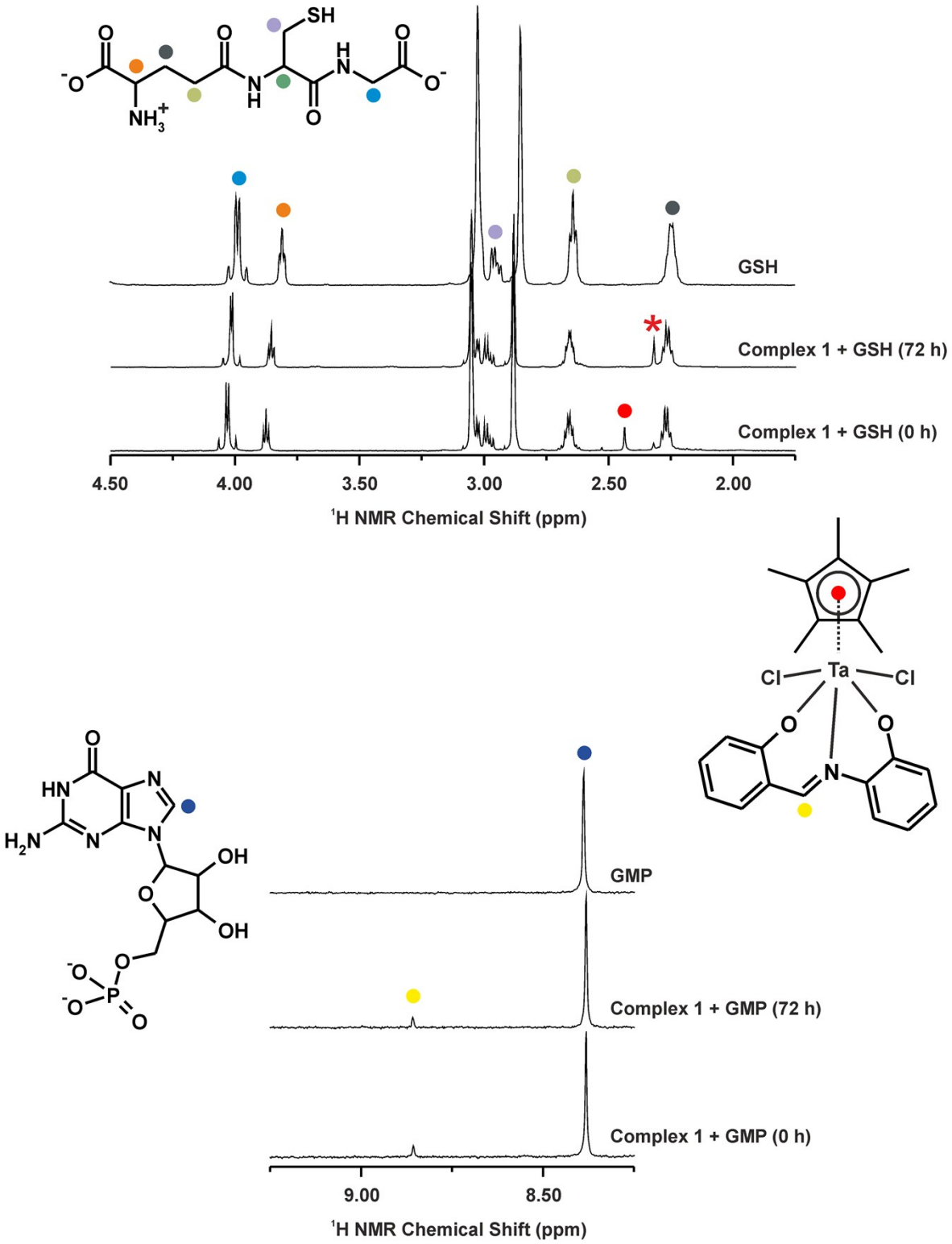

Figure S9. The selected results of ^{1}H NMR studies (50% DMF-d_7/50% D_2O, 37 °C) of the interactions of complex **1** with the reduced glutathione (GSH) or guanosine monophosphate (GMP), given together with the spectra of free biomolecules (for comparative purposes). Red asterisk labels the Cp* signal of **1-OD$_2$**.

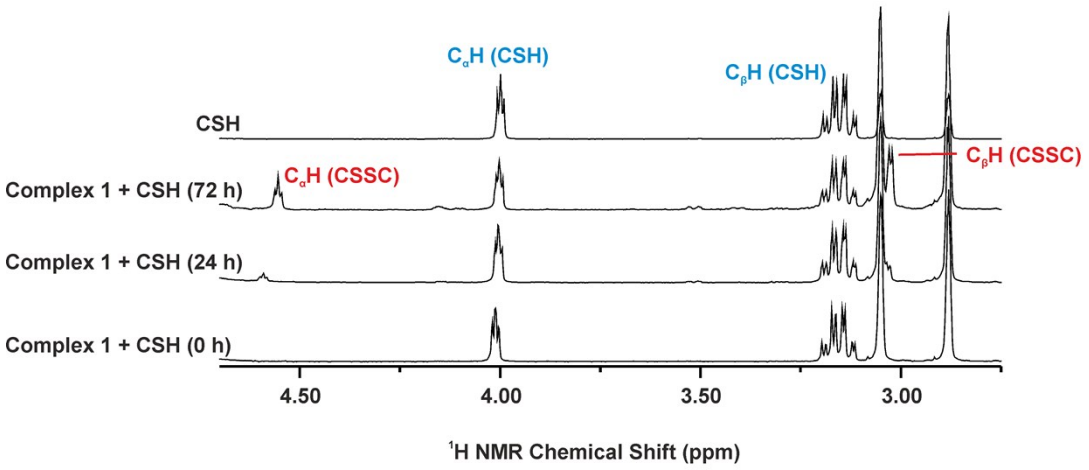

Figure S10. The selected results of ^{1}H NMR studies (50% DMF-d_7/50% D_2O, 37 °C) of the interactions of complex **1** with L-cysteine (CSH) obtained at various time points, given together with the spectrum of free CSH (for comparative purposes).

Table S1. Crystal data and structure refinements for complex **1**.

Empirical formula	$C_{23}H_{24}Cl_2NO_2Ta$
Formula weight	598.28
Temperature (K)	140(2)
Wavelength (Å)	0.71073
Crystal system	Orthorhombic
Space group	$Pna2_1$
a; b; c (Å)	16.8270(12); 14.9556(10); 8.5588(6)
α; β; γ (°)	90.0; 90.0; 90.0
V (Å^3)	2153.9(3)
Z, D_{calc} (g cm^{-3})	4, 1.845
Absorption coefficient (mm^{-1})	5.371
Crystal size (mm)	0.180 × 0.120 × 0.120
F (000)	1168
θ range for data collection (°)	2.421 to 24.994
Index ranges (h; k; l)	$-20 \le h \le 20$; $-17 \le k \le 17$; $-10 \le l \le 10$
Reflections collected	23448
Independent reflections	3784 [R(int) = 0.1107]
Data/restraints/parameters	3784/1/267
Goodness–of–fit on F^2	1.015
Final R indices [$I>2\sigma(I)$]	R_1 = 0.0475, wR_2 = 0.1055
R indices (all data)	R_1 = 0.0611, wR_2 = 0.1103
Largest peak and hole (e Å^{-3})	2.631 and -1.960

Table S2. Selected bond lengths (Å) and angles (°) of complex [Ta(η^5-Cp*)(salaph)Cl$_2$] (**1**) and structurally similar complexes [Ta(η^5-Cp*)(L^1)Cl$_2$]·C$_7$H$_8$ and [Ta(η^5-Cp*)(L^2)Cl$_2$]; H$_2$L^1 = pyridine-2,6-dicarboxylic acid, H$_2$L^2 = 2,6-bis-(hydroxymethyl)pyridine.[14]

	1	[Ta(η^5-Cp*)(L^1)Cl$_2$][a]	[Ta(η^5-Cp*)(L^1)Cl$_2$][a]
Ta–Cl(1)	2.432(6)	2.421(2)	2.463(2)
Ta–Cl(2)	2.427(5)	2.414(2)	2.4978(14)
Ta–O(1)	1.936(10)	2.043(4)	1.953(4)
Ta–O(2)	1.979(11)	2.025(3)	1.937(4)
Ta–N(1)	2.28(2)	2.159(4)	2.174(3)
Ta–C(15)	2.42(2)	2.436(5)	2.448(5)
Ta–C(16)	2.46(2)	2.437(6)	2.446(4)
Ta–C(17)	2.505(14)	2.450(6)	2.481(4)
Ta–C(18)	2.48(2)	2.466(6)	2.503(6)
Ta–C(19)	2.44(3)	2.441(5)	2.485(4)
Ta–Cg	2.1477(8)	2.1286(2)	2.1613(7)
Cl(1)–Ta–Cl(2)	150.4(2)	151.14(6)	152.02(4)
Cl(1)–Ta–O(1)	87.4(4)	85.01(13)	85.54(10)
Cl(1)–Ta–O(2)	87.2(4)	86.61(11)	87.81(11)
Cl(1)–Ta–N(1)	75.6(4)	75.49(12)	76.39(10)
Cl(1)–Ta–Cg	104.8(2)	104.07(4)	103.94(3)
Cl(2)–Ta–O(1)	85.9(3)	84.54(13)	84.71(9)
Cl(2)–Ta–O(2)	87.0(4)	87.55(13)	86.74(10)
Cl(2)–Ta–N(1)	74.9(4)	73.51(15)	75.74(8)
Cl(2)–Ta–Cg	104.76(12)	104.72(4)	103.96(3)
O(1)–Ta–O(2)	155.3(4)	146.79(14)	148.0(2)
O(1)–Ta–N(1)	81.2(5)	73.3(2)	74.22(13)
O(1)–Ta–Cg	101.6(3)	107.47(12)	106.32(9)
O(2)–Ta–N(1)	74.1(5)	73.51(15)	73.8(2)
O(2)–Ta–Cg	103.0(3)	105.74(10)	105.62(10)
N(1)–Ta–Cg	177.1(4)	179.13(12)	179.37(9)

a) different labels than in CIF files (CCDC 714262 and 254685) were used for some atoms in table, in particular: C(15) in Table S2 = C(8) in the CIF files; C(16) = C(9); C(17) = C(10); C(18) = C(11) and C(19) = C(12).

Note: Significant differences were detected in some bond lengths and angles in [Ta(η^5-Cp*)(L^1)Cl_2]·C_7H_8 and [Ta(η^5-Cp*)(L^2)Cl_2] as compared with complex **1**. For example, the Ta–N(1) bond length of complex **1** (see above) is markedly longer than for complexes [Ta(η^5-Cp*)Cl_2(L^1)]·C_7H_8 (2.159(4) Å) and [Ta(η^5-Cp*)Cl_2(L^2)] (2.174(3) Å). Similarly, the O(1)–Ta–O(2), O(1)–Ta–N(1) and N(1)–Ta–Cg bond angles differ considerably for complex **1** (155.3(4)°, 81.2(5)°, and 177.1(4)°, respectively) as compared with its structural analogues [Ta(η^5-Cp*)Cl_2(L^1)]·C_7H_8 (146.79(14)°, 73.3(2)°, and 179.13(12)°, respectively) and [Ta(η^5-Cp*)Cl_2(L^2)] (148.0(2)°, 74.22(13)°, and 179.37(9)°, respectively). These changes are most likely connected with structural differences of the coordinated tridentate *O*,*N*,*O*-ligands, *i.e.*, a combination of six- and five-membered chelating rings of the asymmetric salaph ligand of complex **1** *versus* two five-membered chelating rings of the symmetric L^1 and L^2 ligands.

Table S3. Selected bond lengths (Å) and angles (°) of non-covalent contacts detected in the crystal structure of complex **1**.

Contact	*d*(D–H) (Å)	*d*(H···A) (Å)	*d*(D–H···A) (Å)	<(D–H···A) (°)
C(4)–H(4A)···Cl(2)^{i}	0.95	2.76	3.63(2)	153.4
C(13)–H(13A)···C(5)^{i}	0.95	2.88	3.82(2)	169.0
C(20)–H(20A)···Cl(2)^{ii}	0.98	2.79	3.59(2)	139.1
C(23)–H(23C)···C(6)^{iii}	0.98	2.89	3.66(2)	136.9

Symmetry codes: i) -x, 1-y, z+0.5; ii) x+0.5, 0.5-y, z; iii) 0.5-x, y-0.5, z-0.5.

Table S4. Solubility of complex **1** in various solvents at 20 °C determined by ICP-MS.

	Solubility
DMSO	> 6.00 g/L
ACN	3.28 g/L
MeOH	2.55 g/L
PBS	1.60 mg/L
Tris-HCl	3.61 mg/L
DMEM	6.42 mg/L
RPMI-1640	2.99 mg/L

Table S5. Hydrolysis rate (in %) of complex **1** determined by ^{1}H NMR experiments (an integration of chemical shifts of C–H signal/s of a Cp* ligand). The experiments were performed without or with an addition of several relevant biomolecules (GSH, CSH, Try, GMP).

Medium	Temperature	Biomolecule	0 h	6 h	24 h	48 h	72 h
50% DMF-d_7/50% D_2O	22 °C	-	0	5	7	14	20
50% DMF-d_7/50% D_2O	37 °C	-	18	82	100	100	100
70% DMF-d_7/30% D_2O	37 °C	-	10	20	36	50	58
90% DMF-d_7/10% D_2O	37 °C	-	5	17	26	35	44
50% DMF-d_7/50% D_2O	37 °C	GSH	20	85	100	100	100
50% DMF-d_7/50% D_2O	37 °C	CSH	55	76	95	100	100
50% DMF-d_7/50% D_2O	37 °C	Try	65	74	95	100	100
50% DMF-d_7/50% D_2O	37 °C	GMP	60	80	100	100	100

Table S6. The results of the *in vitro* cytotoxicity testing (IC_{50}±SD; μM) of complex **1** and reference drugs *cisplatin* and *oxaliplatin* against the human ovarian carcinoma (A2780), *cisplatin*-resistant ovarian carcinoma (A2780R) and osteosarcoma (HOS) cells treated for 24 h, 48 h or 72 h. The IC_{50} values (μM) were calculated from viability curves.

	Exposure time	A2780	A2780R	HOS
Complex **1**	24 h	8.6±0.9	16.0±0.3	16.8±2.0
	48 h	8.4±1.9	–	–
	72h	6.4±0.3	–	–
Cisplatin	24 h	20.1±0.3	34.0±1.4	32.6±2.0
	48 h	13.2±2.8	–	–
	72h	7.4±0.3	–	–
Oxaliplatin	24 h	>25.0	>25.0	>25.0

Table S7. The cell viability level (%) determined by an MTT assay at the non-cancerous MRC-5 (72 h exposure) and Hep (24 h exposure) cells treated by complex **1** and *cisplatin* (for comparative purposes).

	1.0	10.0	25.0	50.0	80.0	100.0
MRC-5						
Complex **1**	99.0±1.5	100.7±4.5	94.5±5.0	63.4±6.8	-	-
Cisplatin	86.5±3.4	47.9±4.9	16.4±2.9	19.3±6.4	-	-
Oxaliplatin	93.0±6.8	70.1±2.1	60.6±6.8	-	-	-
Hep						
Complex **1**	104.5	92.1	-	79.1	-	67.6
Cisplatin	100.0	108.7	99.8	91.4	80.9	-

Table S8. Cell populations (%) in the cell cycle phases (PI/RNase staining) of the A2780 cells treated for 24 h by the IC_{50} concentrations of complex **1** and *cisplatin* (for comparative purposes), given together with negative control (untreated cells). The data are given as arithmetic mean from three independent experiments.

	sub-G_1	G_0/G_1	S	G_2/M
Complex **1**	1.2±0.3	71.0±0.9	10.7±0.5	17.1±0.6
Cisplatin	12.4±4.0	38.8±2.1	28.7±1.9	20.1±0.5
Negative control	0.9±0.1	69.2±2.8	14.5±2.3	15.2±0.9

Table S9. The results (given as % populations) of flow cytometry studies of the induction of apoptosis, studied at the A2780 cells treated for 24 h by the IC_{50} concentrations of complex **1** and *cisplatin*. The untreated A2780 cells were employed as the negative control and the cells treated with *staurosporine* (1 μg/mL) represented the positive control. The data are given as arithmetic mean±SD from three independent experiments. LL, lower left; LR, lower right; UL, upper left; UR, upper right.

	LL quadrant (FL1–/FL3–)	LR quadrant (FL1+/FL3–)	UR quadrant (FL1+/FL3+)	UL quadrant (FL1–/FL3+)
Complex **1**	11.4±0.7	37.2±2.0	47.9±1.7	3.6±0.5
Cisplatin	21.7±1.2	34.2±2.2	39.2±2.6	4.9±1.8
Staurosporine	9.5±2.3	43.0±4.1	41.9±7.1	5.7±1.3
Negative control	89.5±1.2	1.8±0.3	4.3±0.4	4.5±0.6

Table S10. The results (given as % cell populations) of flow cytometry studies of the mitochondrial membrane potential changes, studied at A2780 cells using the treatment by the IC_{50} concentrations of complex **1** for 24 h. *Cisplatin* and *staurosporine* were used for comparative purposes, the untreated A2780 cells represent the negative control, while the CCCP-treated cells were used as the positive control. The data are given as arithmetic mean±SD from three independent experiments.

	% of Cells Showing Low FL-2 Orange Fluorescence
Complex **1**	98.9±0.5
Cisplatin	46.8±7.6
Staurosporine	52.4±2.6
Positive control (CCCP)	89.8±1.6
Negative control	4.0±1.0

Table S11. The results (given as % cell populations) of the cytochrome *c* release studied by flow cytometry at the A2780 cells treated for 24 h by the IC_{50} concentrations of complex **1** (and *cisplatin* and *staurosporine* were used for comparative purposes). The untreated A2780 cells were employed as the negative control, while the cells applied with the Anti-IgG1-FITC Isotype represented the positive control. The data are given as arithmetic means ± SD from three independent experiments.

	% of Cells Showing Low FL-1 Green Fluorescence
Complex **1**	86.1±2.7
Cisplatin	67.9±3.0
Staurosporine	72.8±3.0
Positive control	98.3±0.6
Negative control	0.7±0.2

Table S12. The results (given as % populations) of flow cytometry studies of the induction of total reactive oxygen species (ROS) and superoxide production, studied at A2780 cells using the treatment by the IC_{50} concentrations of complex **1** for 24 h. The untreated A2780 cells were used as the negative control and cells treated with pyocyanine represent the positive control. The data are given as arithmetic mean±SD from three independent experiments. LL, lower left; LR, lower right; UL, upper left; UR, upper right.

	LL quadrant (FL1−/FL2−)	LR quadrant (FL1+/FL2−)	UR quadrant (FL1+/FL2+)	UL quadrant (FL1−/FL2+)
Complex **1**	<0.1	<0.1	97.2±1.2	2.7±1.2
Positive control	<0.1	<0.1	95.8±1.1	4.2±1.0
Negative control	98.6±0.4	0.5±0.2	<0.1	0.8±0.2

References

1 F. Tisato, F. Refosco, U. Mazzi, G. Bandoli and M. Nicolini, *J. Chem. Soc. Dalton Trans.*, 1987, **1987**, 1693.

2 H. E. Gottlieb, V. Kotlyar and A. Nudelman, *J. Org. Chem.*, 1997, **62**, 7512.

3 Bruker. Apex3. Bruker AXS Inc., Madison, Wisconsin, USA (2015).

4 G. M. Sheldrick, *Acta Cryst.*, 2015, **C71**, 3.

5 K. Brandenburg, Diamond Version 4.0.3., Crystal Impact GbR, Bonn, Germany (2015).

6 C. F. Macrae, I. J. Bruno, J. A. Chisholm, P. R. Edgington, P. McCabe, E. Pidcock, L. Rodriguez-Monge, R. Taylor, J. van de Streek and P. A. Wood, *J. Appl. Crystallogr.*, 2008, **41**, 466.

7 V. Velma, S. R. Dasari and P. B. Tchounwou, *Biomark Insights.*, 2016, **11**, 113.

8 R. C. Taylor, S. P. Cullen and S. J. Martin, *Nat. Rev. Mol. Cell Biol.*, 2008, **9**, 231.

9 S. Yoon, S. J. Park, J. H. Han, J. H. Kang, J. H. Kim, J. Lee, S. Park, H. J. Shin, K. Kim, M. Yun and Y. J. Chwae, *Cell Death Dis.*, 2014, **5**, e1494.

10 (*a*) I. Romero-Canelón, M. Mos and P. J. Sadler, *J. Med. Chem.*, 2015, **58**, 7874; (*b*) J. M. Hearn, I. Romero-Canelón, A. F. Munro, Y. Fu, A. M. Pizarro, M. J. Garnett, U. McDermott, N. O. Carragher and P. J. Sadler, *Proc. Natl. Acad. Sci. USA*, 2015, **112**, E3800.

11 L. Kelland, *Nature Rev. Cancer*, 2007, **7**, 573.

12 S. M. Meier, D. Kreutz, L. Winter, M. H. M. Klose, K. Cseh, T. Weiss, A. Bileck, B. Alte, J. C. Mader, S. Jana, A. Chatterjee, A. Bhattacharyya, M. Hejl, M. A. Jakupec, P. Heffeter, W. Berger, C. G. Hartinger, B. K. Keppler, G. Wiche and C. Gerner, *Angew. Chem. Int. Ed.*, 2017, **56**, 8267.

13 S. J. Shin, J. A. Smith, G. A. Rezniczek, S. Pan, R. Chen, T. A. Brentnall, G. Wiche and K. A. Kelly, *Proc. Natl. Acad. Sci. USA*, 2013, **110**, 19414.

14 (*a*) A. Conde, R. Fandos, A. Otero and A. Rodríguez, Organometallics, 2008, **27**, 6090; (*b*) R. Fandos, I. López-Solera, A. Otero, A. Rodríguez and M. J. Ruiz, Organometallics, 2004, **23**, 5030.